CONSTRAINTS FROM LABORATORY EXPERIMENTS ON CRATER EXCAVATION AND FORMATION OF AN UPRANGE FORBIDDEN ZONE IN AN OBLIQUE IMPACT. R. R. Herrick[1], S. Yamamoto[2], O. S. Barnouin-Jha[3], S. Sugita[2], and T. Matsui[2], [1]Geophysical Institute, University of Alaska Fairbanks, Fairbanks, AK 99775-7320 (rherrick@gi.alaska.edu); [2]Dept. of Complexity Science and Engineering, University of Tokyo, Japan; [3]The Johns Hopkins University Applied Physics Laboratory, Laurel, MD.

Introduction: Planetary impacts occur primarily at nonvertical angles, and craters that form from the lowest impact angles have an uprange forbidden zone in the ejecta that appears as an outward curving "V" (Fig. 1) [1,2]. Early experimental work [2] successfully mimicked the ejecta planforms of planetary craters and presented downrange and crossrange topographic profiles of low-angle impacts. That work associated asymmetry in the ejecta planform with early-time downrange tilting of the cone of the ejecta curtain. Subsequent numerical modeling and experimental work has begun to document the asymmetries in shock-wave propagation, ejection velocities, and ejection angles associated with oblique impact [3,4,5,6,7]. In particular, a series of experiments imaged with the 3D PIV technique provided details of the azimuthal variation of ejecta velocity and angle as the ejecta curtain developed for a variety of impact angles [5,6]. This technique provides less information on the azimuthal variation of the amount of ejected material.

In 2005 we conducted a series of impact experiments at the Department of Complexity Science, University of Tokyo Kashiwa. Details of the experimental setup are presented in [8]. These experiments, conducted at a variety of impact angles, were designed to provide enough information to delineate the distribution of the final ejecta at a higher level of detail than published in [2]. We also have movies of crater excavation imaged at surface level in a direction roughly perpendicular to the projectile direction. Our goal is to utilize the data we collected in concert with published results [e.g., 3,4,5,6] to assess the nature and relative importance of possible contributing factors in producing the observed uprange forbidden zones. If we conceptualize crater excavation as an expanding cone-shaped flow through the pre-impact surface, then from [5,6] we identify the following potential contributors to the final ejecta distribution and production of an uprange zone of avoidance in our experiments: a) tilting of the ejecta cone (esp. downrange); b) movement of the cone center (esp. downrange); c) changing the interior slope of the cone with time and azimuth (esp. becoming elliptical); d) azimuthal variation in velocity of material in the cone (esp. higher velocities downrange); and e) azimuthal variation in cone density (esp. an ejecta-free uprange section). For hypervelocity impacts additional factors such as melting and vaporization of impactor/target material may also play a role in establishing the final ejecta pattern.

Methodology: The experiments were conducted at ~200 m/s in a vacuum with polycarbonate projectiles impacting a sand target. The sand was covered with a dusting of flour so that it is easy to identify the extent of the continuous ejecta in the final images. In Fig. 2 we show images of the ejecta for a vertical impact versus a 20-degree impact that shows a well-developed forbidden zone. We have scaled the images so that the craters have the same diameter. The continuous ejecta extends ~1 R from the crater rim for the vertical impact. In Fig. 3 we show the azimuthal variation of the scaled maximum extent of the ejecta for the oblique impact relative to the mean for the vertical impact.

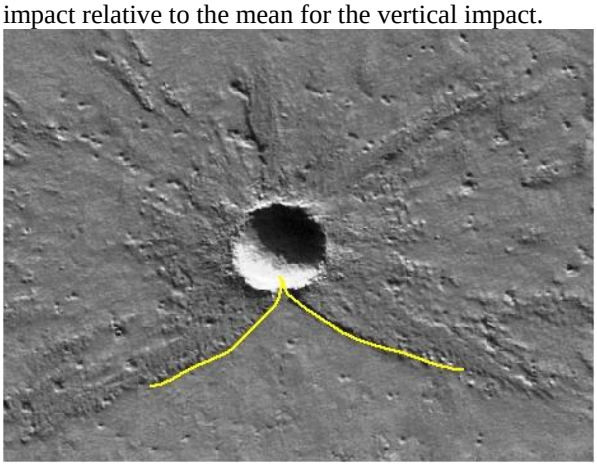

Fig. 1. Crater 280 m in diameter on Mars (86.3 S, 247 E) with uprange forbidden zone in shape of outward curving "V"; inferred projectile direction of travel is up the page.

Utilizing hand-held digital photographs of the craters taken at two look angles, we can use simple photogrammetric techniques to generate a digital elevation model (DEM) for the final crater. Fig. 4 shows a DEM of the 20-degree impact along with extracted profiles. A DEM of the experimental craters allows us to assess the azimuthal variation of ejected material.

To summarize, our data provides a record of the azimuthal variation of the ejecta, and we have this data for a full spectrum of impact angles. We hope to synthesize our data with previous work to understand how the excavation flow evolves during an oblique impact.

Discussion: If we compare the maximum extent of the continuous ejecta (Figs 2 & 3) with the ejection velocities and angles for highly oblique impacts in [5,6], then it appears that the variation in factors a-d discussed above are not adequate to produce the uprange zone of avoidance. It seems that there is no ejecta in the uprange direction at any velocity or angle

for a significant portion of the excavation process. Initially there is a missing uprange wedge in the ejecta cone as excavation begins. The size of the wedge decreases as excavation continues, and this is the primary factor producing the outward curving V that is observed. The azimuthal variation in ejecta extent, rim elevation, and rim width indicates that there must also be variation in the amount of material in the cone (more crossrange) throughout excavation.

Continued processing of the experimental data for the spectrum of impact angles will allow us to assess the full progression of ejecta flow from vertical to near-horizontal impact.

References: [1] Herrick R.R and Hessen K.K (2006) *MAPS* 41:1483-1495. [2] Gault D.E. and Wedekind J.A. (1978) *Proc. LPSC 9th*, 3843-3875. [3] Pierazzo E. and Melosh H.J. (2000) *Ann. Rev. Earth and Planet. Sci.* 28:141-167. [4] Dahl J.M. and Schultz P.H. (2001) *Int. J. Imp. Eng.* 26:145-155. [5] Anderson J.L.B. et al. (2004) *MAPS* 39:303-320. [6] Anderson J.L.B. et al. (2003) *JGR* doi:10.10292003/JE002075. [7] Yamamoto S. et al. (2005) *Icarus* 178:264-273. [8] Hessen et al. (2007) *LPS XXXVIII* Abs. 2141.

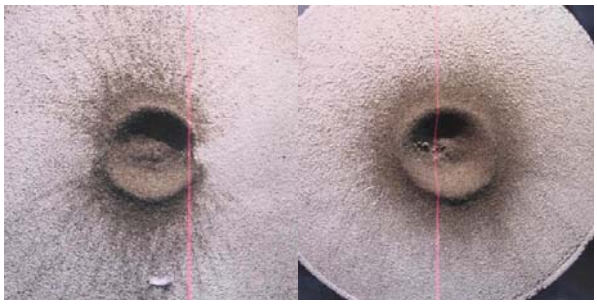

Fig. 2. Images of 20-degree (left) and vertical impacts scaled to same crater diameter (downrange to left).

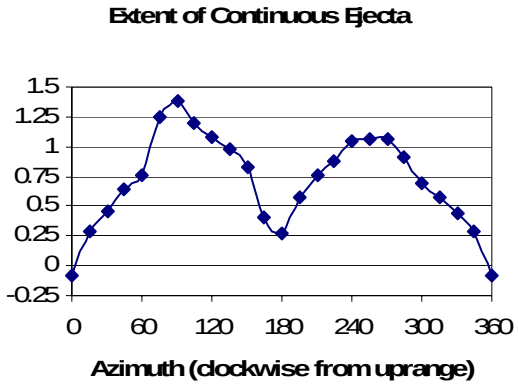

Fig. 3. Maximum extent of the continuous ejecta for the 20-degree impact relative to the mean for the vertical impact after scaling craters to the same diameter.

Fig. 4 (to right). Topography of 20-degree impact along with profiles downrange, crossrange, and tracing the perimeter of the rim. All units are millimeters.